

growth-promoting activity of Tax (24–26). However, it should be noted that no Tax or Env proteins could be detected in the joints by both immunoblotting and immunohistochemical techniques. This is probably due to low amounts of the proteins, because the mRNA level of these proteins was low even in the affected joints, being approximately 1/2000 of that detected in MT-2 cells. Nonetheless, the observation that the amounts of HTLV-I mRNA expression in affected joints were five to ten times higher than in apparently normal mice suggests a correlation between the RNA expression and the joint disease. Probably, small amounts of Tax are enough to exert an influence on cells at the joint.

Another possible explanation for the induction of inflammatory arthropathy is an immunological disturbance by the transgene. The observation that some of the mice had antibodies to immunoglobulins and DNAs suggests autoimmune-like complications in these mice. Although exocrine pathology resembling Sjögren's syndrome, a presumed autoimmune disease, has been found in *tax* transgenic mice (27), our transgenic mice showed no abnormalities in the salivary and lachrymal glands. The possibil-

ity that an immune reaction could be induced against synovial cells expressing viral antigens or antigens cross-reactive with viral antigens seems less likely; no antibodies to HTLV-I antigens have been detected in these transgenic mice, and no cross-reactivity of the Env and pX antigens with rheumatoid synovium is known. Gag does cross-react with rheumatoid synovium, but it is not carried by these transgenic mice (28). In any event, these transgenic mice should provide a useful model to investigate the development of rheumatoid arthritis in humans.

#### REFERENCES AND NOTES

1. J. L. Decker *et al.*, *Ann. Intern. Med.* **101**, 810 (1984).
2. A. M. Krieg and A. D. Steinberg, *J. Autoimmunity* **3**, 137 (1990).
3. T. Koga *et al.*, *Infect. Immun.* **50**, 27 (1985).
4. M. F. Van Den Broek *et al.*, *J. Exp. Med.* **170**, 449 (1989).
5. W. Van Eden *et al.*, *Proc. Natl. Acad. Sci. U.S.A.* **82**, 5117 (1985).
6. B. C. Cole and G. H. Cassell, *Arthritis Rheum.* **22**, 1375 (1975).
7. I. Kitajima *et al.*, *ibid.* **32**, 1344 (1989).
8. H. Sabe *et al.*, *Int. J. Cancer* **41**, 880 (1988).
9. Y. Iwakura *et al.*, unpublished data.
10. S. M. Krane, in *Arthritis*, D. J. McCarty, Ed. (Lea and Febiger, Philadelphia, 1985), pp. 593–604.
11. M. Takiguchi and Y. Iwakura, unpublished observation.
12. L. Hang, A. N. Theofilopoulos, F. J. Dixon, *J. Exp. Med.* **155**, 1690 (1982).
13. K. Nishioka *et al.*, *Lancet* **i**, 441 (1989).
14. W. P. Cheevers *et al.*, *Lab. Invest.* **58**, 510 (1988).
15. R. Winchester *et al.*, *Ann. Intern. Med.* **106**, 19 (1987).
16. L. R. Espinoza *et al.*, *Arthritis Rheum.* **31**, 1034 (1988); J. Bentin *et al.*, *ibid.* **33**, 268 (1990).
17. B. K. Felber *et al.*, *Science* **229**, 675 (1985).
18. M. Maruyama *et al.*, *Cell* **48**, 343 (1987).
19. M. Fujii, P. Sassone-Corsi, I. M. Verma, *Proc. Natl. Acad. Sci. U.S.A.* **85**, 8526 (1988).
20. W. P. Arend and J. M. Dayer, *Arthritis Rheum.* **33**, 305 (1990).
21. M. Tosu and Y. Iwakura, unpublished observation.
22. Y. Wano *et al.*, *J. Clin. Invest.* **80**, 911 (1987).
23. N. Miyasaka *et al.*, *J. Autoimmunity*, in press.
24. A. Tanaka *et al.*, *Proc. Natl. Acad. Sci. U.S.A.* **87**, 1071 (1990).
25. M. Nerenberg *et al.*, *Science* **237**, 1324 (1987).
26. S. H. Hinrichs, M. Nerenberg, R. K. Reynolds, G. Khoury, G. Jay, *ibid.*, p. 1340.
27. J. E. Green *et al.*, *Nature* **341**, 72 (1989).
28. B. Ziegler, G.-Q. Huang, R. E. Gay, H.-G. Fassbender, S. Gay, *Arthritis Rheum.* **31**, S35 (1988).
29. D. A. Melton *et al.*, *Nucleic Acids Res.* **12**, 7035 (1984).
30. J. M. Chirgwin, A. E. Przybyla, R. J. MacDonald, W. J. Rutter, *Biochemistry* **18**, 5294 (1979).
31. Y. Iwakura, M. Asano, Y. Nishimune, Y. Kawade, *EMBO J.* **7**, 3757 (1988).
32. We thank H. Shibuta for valuable discussion, H. Nagashima, M. Hayashi, and N. Hayashi for animal care, and S. Ueda and T. Nuroya at the Nippon Institute for Biological Science for examination of pathological specimens. This work was supported by grants from the Ministry of Education, Science, and Culture of Japan.

14 December 1990; accepted 29 May 1991

## Identification of a Site in Glutamate Receptor Subunits That Controls Calcium Permeability

RICHARD I. HUME, RAYMOND DINGLEDINE, STEPHEN F. HEINEMANN\*

The neurotransmitter glutamate mediates excitatory synaptic transmission throughout the brain. A family of genes encoding subunits of the non-N-methyl-D-aspartate (non-NMDA) type of glutamate receptor has been cloned. Some combinations of these subunits assemble into receptors with a substantial permeability to calcium, whereas others do not. To investigate the structural features that control ion permeation through these ligand-gated channels, mutant receptor subunits with single-amino acid changes were constructed. Mutation of a certain amino acid that results in a net charge change (from glutamine to arginine or vice versa) alters both the current-voltage relation and the calcium permeability of non-NMDA receptors. A site has thus been identified that regulates the permeation properties of these glutamate receptors.

**I**NFLUX OF CA THROUGH GLUTAMATE receptors (GluR) is thought to play a key role in long-term potentiation, excitotoxic neuron damage, and epilepsy (1). In many neurons, non-NMDA glutamate

receptors have low permeability to  $\text{Ca}^{2+}$  (2). However, in a few types of neurons,  $\text{Ca}^{2+}$  influx through non-NMDA receptor channels is more pronounced (3). The four subunits of the first family of non-NMDA glutamate receptors to be cloned (4–6), named GluR1, GluR2, GluR3, and GluR4 (7), are similar to one another in amino acid sequence. When expressed in *Xenopus* oocytes alone or in combination, GluR1 and GluR3 form receptors that have a substantial  $\text{Ca}^{2+}$  permeability, but when GluR2 is coexpressed with either GluR1 or GluR3, the receptor channels have little or no  $\text{Ca}^{2+}$  permeability (8). The current-voltage (*I-V*)

relations of these subunit combinations are also distinct. GluR1 or GluR3 receptor channels display a strongly inwardly rectifying *I-V* relation, whereas these subunits coassembled with GluR2 have a linear or outwardly rectifying *I-V* relation (5, 6).

To determine the regions of these proteins that are responsible for the permeation properties of the channels, we first examined the functional properties of subunit chimeras. These experiments indicated that a region extending from the middle of the  $\text{NH}_2$ -terminal extracellular domain through the third putative transmembrane segment determined the shape of the *I-V* curve (9). In this region, the amino acid sequence similarities of GluR1, GluR2, and GluR3 are high. We searched for positions in this region in which the corresponding amino acid is the same in GluR1 and GluR3 but different in GluR2 and found one charge substitution in a region of otherwise identical amino acid sequence (Fig. 1A). In this region, a glutamine is present in GluR1 and GluR3, the two subunits with rectifying *I-V* relations, whereas arginine resides in the equivalent position of GluR2, the subunit that can combine to form receptors with linear *I-V* relations. This charge difference is near one end of a sequence that has been postulated to form the second membrane-spanning domain (6) or an extracellular loop

R. I. Hume, Molecular Neurobiology Laboratory, Salk Institute, La Jolla, CA 92037, and Department of Biology, University of Michigan, Ann Arbor, MI 48109.  
R. Dingleline, Molecular Neurobiology Laboratory, Salk Institute, La Jolla, CA 92037, and Department of Pharmacology, University of North Carolina, Chapel Hill, NC 27599.  
S. F. Heinemann, Molecular Neurobiology Laboratory, Salk Institute, La Jolla, CA 92037.

\*To whom correspondence should be addressed.

(4). To test the importance of this charge substitution, we made two complementary mutant receptor subunits, using standard methods for site-directed mutagenesis (10). In one mutant, GluR2(R607Q), the arginine in GluR2 was converted to glutamine so that the mutant resembled GluR1 and GluR3. In the second mutant, GluR3(Q612R), the glutamine in GluR3 was converted to an arginine so that the mutant resembled GluR2. These single amino acid changes had large and reciprocal effects.

Although it differed from the wild-type GluR3 by only a single amino acid, GluR3-(Q612R) had different properties than its wild-type parent did when expressed in *Xenopus* oocytes (11). Wild-type GluR3 RNA expressed by itself produced robust responses (often greater than 1  $\mu$ A at  $-100$  mV), but we observed little kainate-evoked current when RNA encoding GluR3(Q612R) was injected into oocytes (range 0 to 3 nA,  $n = 9$ ). However, this mutant was functional because, when coexpressed with GluR1,

the  $I$ - $V$  relation was linear, rather than inwardly rectifying (Fig. 1B). Thus, this GluR3 mutant has a phenotype like that of GluR2. Changing the corresponding single amino acid in GluR2 altered the properties of receptors in the reciprocal manner. Whereas the parent GluR2 itself was nearly inactive when expressed alone, GluR2-(R607Q) receptors responded to kainate with large inwardly rectifying currents (Fig. 1B) like those of GluR1 and GluR3. Thus, this mutant GluR2 subunit behaves like GluR3 and GluR1, rather than like the parent GluR2. A convenient and sensitive measure of the degree of rectification is the ratio of kainate-induced slope conductances at positive and negative potentials (12). The index of rectification ( $g_{+40}/g_{-75}$ ) was virtually zero for GluR2(R607Q) or GluR1 plus GluR2(R607Q) receptors, as it was for wild-type GluR1 plus GluR3 receptors (Fig. 1C). Conversely, when GluR1 was coexpressed with either the mutant GluR3 subunit or wild-type GluR2, the resulting receptors displayed a conductance ratio near 1.5.

The mutations that altered the  $I$ - $V$  relation of these non-NMDA receptors also altered the  $\text{Ca}^{2+}$  permeability of their channels. We examined the  $\text{Ca}^{2+}$  permeability of the mutant subunits by bathing oocytes in solutions in which most of the  $\text{Na}^+$  had been removed and in which the concentration of divalent cation ( $\text{Ca}^{2+}$  or  $\text{Ba}^{2+}$ ) had been raised to 60 mM. If the receptor channel is permeable only to monovalent cations, the shift in reversal potential as the normal solution is changed to a low  $\text{Na}^+$  solution with high divalent cation concentration would be  $-60$  mV. If divalent cations such as  $\text{Ca}^{2+}$  can also cross the membrane, the shift in reversal potential would be less negative or positive if the permeability to divalent cations is sufficiently large.

For all combinations of subunits tested, the inward current at  $-100$  mV was smaller in solutions with high  $\text{Ba}^{2+}$ , low  $\text{Na}^+$  concentrations than in the standard solution. However, the shape of the  $I$ - $V$  curve in this solution depended on the subunit composition. When oocytes expressing both GluR1 and GluR3(Q612R) were bathed in a solution with high  $\text{Ba}^{2+}$  and low  $\text{Na}^+$  concentrations (Figs. 2A and 3), the kainate-evoked currents reversed polarity at a substantially more negative potential ( $-46 \pm 1.8$  mV, mean  $\pm$  SEM,  $n = 5$ ) than they did in standard solution ( $-9 \pm 0.6$  mV,  $n = 13$ ). This large, negative shift in reversal potential reflects a channel that is permeable mainly to monovalent cations. In the high  $\text{Ba}^{2+}$  and low  $\text{Na}^+$  solution, the reversal potential of oocytes coexpressing GluR1 and GluR3(Q612R) was similar to that for

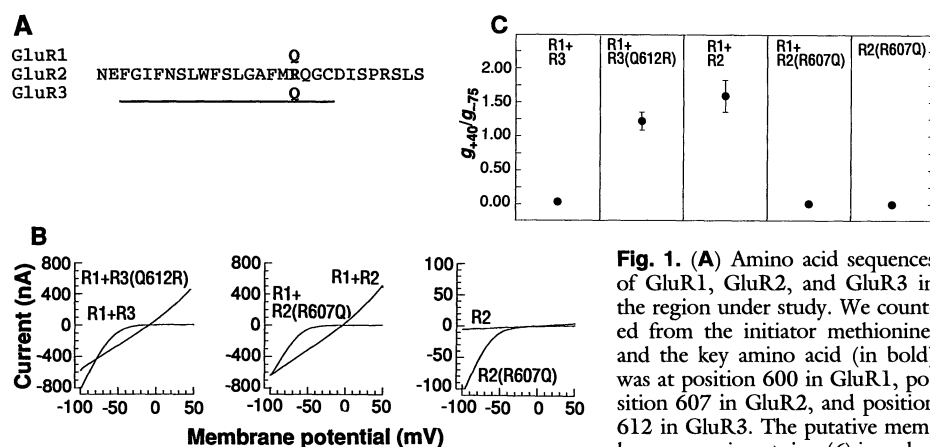


**Fig. 1.** (A) Amino acid sequences of GluR1, GluR2, and GluR3 in the region under study. We counted from the initiator methionine, and the key amino acid (in bold) was at position 600 in GluR1, position 607 in GluR2, and position 612 in GluR3. The putative membrane-spanning region (6) is underlined. (B)  $I$ - $V$  relations for individual oocytes injected with RNA encoding combinations of wild-type and mutant glutamate receptors (11). (C) Index of rectification in  $I$ - $V$  relations for a series of oocytes injected with wild-type and mutant RNAs. For each cell, the slope conductance ( $g$ ) was measured at  $+40$  mV ( $g_{+40}$ ) and at  $-75$  mV ( $g_{-75}$ ) (12), and the ratio was taken. Cells with pronounced inward rectification have a ratio near 0. Each panel of the figure shows the average ratio from 4 to 20 cells  $\pm$  SEM. For some points, the error bars were smaller than the symbols.

lined. The single amino acid code is as follows: N, asparagine; E, glutamate; F, phenylalanine; G, glycine; I, isoleucine; S, serine; L, leucine; W, tryptophan; A, alanine; M, methionine; R, arginine; Q, glutamine; C, cysteine; D, aspartate; and P, proline. (B)  $I$ - $V$  relations for individual oocytes injected with RNA encoding combinations of wild-type and mutant glutamate receptors (11). (C) Index of rectification in  $I$ - $V$  relations for a series of oocytes injected with wild-type and mutant RNAs. For each cell, the slope conductance ( $g$ ) was measured at  $+40$  mV ( $g_{+40}$ ) and at  $-75$  mV ( $g_{-75}$ ) (12), and the ratio was taken. Cells with pronounced inward rectification have a ratio near 0. Each panel of the figure shows the average ratio from 4 to 20 cells  $\pm$  SEM. For some points, the error bars were smaller than the symbols.

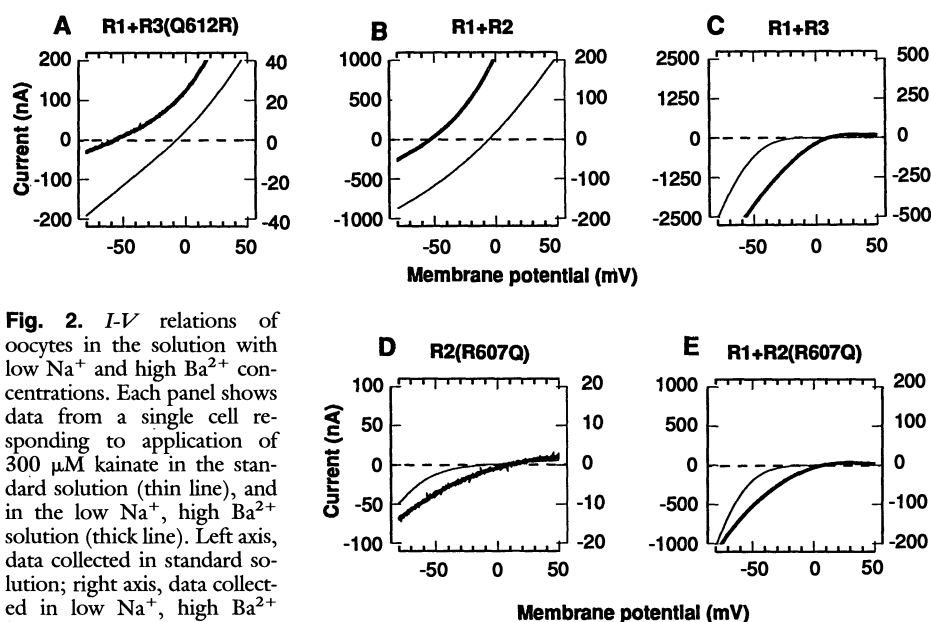


**Fig. 2.**  $I$ - $V$  relations of oocytes in the solution with low  $\text{Na}^+$  and high  $\text{Ba}^{2+}$  concentrations. Each panel shows data from a single cell responding to application of 300  $\mu$ M kainate in the standard solution (thin line), and in the low  $\text{Na}^+$ , high  $\text{Ba}^{2+}$  solution (thick line). Left axis, data collected in standard solution; right axis, data collected in low  $\text{Na}^+$ , high  $\text{Ba}^{2+}$  solution. Oocytes were bathed in the standard solution (11) or in a solution containing 60 mM  $\text{BaCl}_2$ , 1 mM KCl, and 15 mM Hepes. We added approximately 8 mM Na as NaOH to adjust the pH to 7.5. (A) GluR1 plus GluR3(Q612R) receptors; (B) wild-type GluR1 plus GluR2 receptors; (C) wild-type GluR1 plus GluR3 receptors; (D) homomeric GluR2(R607Q) receptors; and (E) GluR1 plus GluR2(R607Q) receptors.

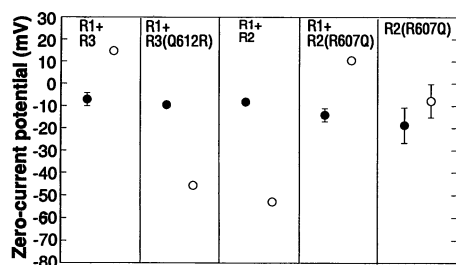


**Fig. 3.** Average reversal or zero-current potential of oocytes bathed in standard solution (solid dots) or in the low  $\text{Na}^+$ , high  $\text{Ba}^{2+}$  solution (open dots). Each panel of the figure shows the average of three to six cells  $\pm$  SEM. For some points, the error bars were smaller than the symbols.

wild-type GluR1 plus GluR2 receptors ( $-53 \pm 0.8$  mV,  $n = 5$ ; Figs. 2B and 3). Furthermore, the  $I$ - $V$  relationship of these receptors showed pronounced outward rectification in the solution with high  $\text{Ba}^{2+}$  and low  $\text{Na}^+$  concentrations, as would be expected for a process that allowed predominantly monovalent cations to permeate (Fig. 2, A and B).

The left shift of the  $I$ - $V$  curve of GluR1 plus GluR3(Q612R) that results when most of the  $\text{Na}^+$  was replaced by  $\text{Ba}^{2+}$  (Fig. 2A) contrasts with the right shift of the  $I$ - $V$  curve of receptors assembled from GluR1 plus wild-type GluR3 (Fig. 2C) (8). This right shift in the  $I$ - $V$  curve indicates that the wild-type channel has a substantial  $\text{Ba}^{2+}$  permeability. When precautions were taken to minimize the secondary activation of  $\text{Ca}^{2+}$ -dependent  $\text{Cl}^-$  currents (13), we found that this combination of subunits showed extreme rectification in the low  $\text{Na}^+$ , high  $\text{Ba}^{2+}$  solution, as well as in the high  $\text{Na}^+$ , low  $\text{Ca}^{2+}$  solution. Because a clear reversal from inward to outward current was not always obtained, we define the "zero current potential" as the most negative potential at which inward current was negligible. For GluR1 plus wild-type GluR3 receptors, the average zero current potential shifted from  $-7 \pm 2.9$  mV to  $+15 \pm 1.6$  mV ( $n = 6$ ) when  $\text{Ba}^{2+}$  replaced  $\text{Na}^+$  (Fig. 3).

As was the case for the  $I$ - $V$  relation, the arginine-to-glutamine mutation in GluR2 had the opposite effect of the glutamine-to-arginine mutation in GluR3. Oocytes expressing GluR2(R607Q) alone, or GluR1 plus GluR2(R607Q), produced kainate responses that approached zero current at potentials near 0 mV in the solution with high  $\text{Ba}^{2+}$  and low  $\text{Na}^+$  concentrations (Fig. 2, D and E, and Fig. 3). These zero current potentials are substantially more positive than the reversal potential for  $\text{Cl}^-$  ( $-32$  mV) (14) or monovalent cations ( $-65$  mV) and must therefore represent entry of

$\text{Ba}^{2+}$  through the glutamate receptors.

When these experiments were repeated with  $\text{Ca}^{2+}$  as the charge carrier, the results were consistent with those obtained in  $\text{Ba}^{2+}$ , confirming that there was a substantial  $\text{Ca}^{2+}$  permeability through subunit combinations containing a mutant GluR2. In high  $\text{Ca}^{2+}$  concentrations, however, kainate responses were contaminated by secondary activation of endogenous  $\text{Cl}^-$  currents. In 60 mM  $\text{Ca}^{2+}$ , for example, the zero-current potentials of GluR1 plus GluR2(R607Q) and of GluR2(R607Q) expressed alone were  $-22 \pm 2.7$  mV ( $n = 3$ ) and  $-20$  mV ( $n = 2$ ), respectively. This was still substantially more positive than the equilibrium potential for monovalent cations in this solution (reversal potential for GluR1 plus GluR2 was  $-48$  mV) but close to the equilibrium potential for  $\text{Cl}^-$  ( $-25$  mV) (14).

If we assume that all monovalent cations are equally permeant and that the responses we have measured are uncontaminated by  $\text{Cl}^-$  currents, we can use the magnitude of the shift in reversal potential to estimate the permeability ratio of  $\text{Ba}^{2+}$  to monovalent cations. The negative shift in reversal potential when  $\text{Na}^+$  is replaced by  $\text{Ba}^{2+}$  that is characteristic of GluR1 plus GluR2 receptors or GluR1 plus GluR3(Q612R) receptors indicates a  $\text{Ba}^{2+}$  to monovalent permeability ratio in the range of 0.01 to 0.05. This is similar to the  $\text{Ca}^{2+}$  to  $\text{Na}^+$  permeability ratio calculated for kainate-activated receptors on cultured hippocampal neurons (2). In contrast, if the zero current potential of GluR1 plus GluR2(R607Q) receptors is used in this calculation, the  $\text{Ba}^{2+}$  to monovalent permeability ratio is in the range of 1 to 3 (15). This value is less than the value of about 8 estimated for the NMDA channel in cultured hippocampal neurons (2) but indicates that the divalent ion permeability of receptors with inwardly rectifying  $I$ - $V$  relations is at least 30-fold higher than that for receptors with outwardly rectifying  $I$ - $V$  relations.

We have identified a site that appears to be a key regulator of ion permeation through non-NMDA receptor channels. When this site contains an arginine, the resulting receptors carry little current by themselves, but when coexpressed with other subunits, the receptors exhibit a linear  $I$ - $V$  relation and low  $\text{Ca}^{2+}$  permeability. When the site contains a glutamine, the protein can self-assemble into functional receptors that allow  $\text{Ca}^{2+}$ , as well as monovalent cations, to cross the membrane. This region is therefore likely to be in or near the ion permeation path of the activated receptor channel. These results suggest an explanation for the weak ability of homomeric GluR2 or

GluR3(Q612R) channels to carry current: the homomeric assembly of subunits that each carry a positive charge in or near the channel could interfere with cation permeation. Similarly, the inward rectification of GluR1, GluR3, and GluR2(R607Q) channels might be explained by their having a high  $\text{Ca}^{2+}$  permeability if, for example, the absence of the positively charged arginine unmasks a binding site for divalent ions in the channel. The positive charge of arginine could neutralize a carbonyl or ionized carboxyl group that forms part of a divalent ion binding site. Alternatively, the presence of the positively charged arginine in or near the channel might select against the permeation of the divalent cations in an otherwise weakly selective channel.

*Note added in proof:* Verdoorn and co-workers (21) recently reported results similar to those shown in Fig. 1. They identified the same arginine to glutamine switch, but they used a different nomenclature and amino acid numbering convention than used here (7).

#### REFERENCES AND NOTES

1. D. V. Madison *et al.*, Nicoll, *Annu. Rev. Neurosci.* **14**, 379 (1991); R. Dingledine *et al.*, *Trends Pharmacol. Sci.* **11**, 334 (1990); D. T. Monaghan *et al.*, *Annu. Rev. Pharmacol. Toxicol.* **29**, 365 (1989); R. G. M. Morris *et al.*, *Philos. Trans. R. Soc. London Ser. B* **329**, 187 (1990); D. W. Choi, *Neuron* **1**, 623 (1988).
2. M. L. Mayer and G. L. Westbrook, *Prog. Neurobiol. (NY)* **28**, 197 (1987).
3. S. N. Murphy *et al.*, *J. Neurosci.* **7**, 4145 (1987); M. Iino *et al.*, *J. Physiol. (London)* **424**, 151 (1990); T. A. Gilbertson *et al.*, *Science* **251**, 1613 (1991).
4. M. Hollmann, A. O'Shea-Greenfield, S. W. Rogers, S. F. Heinemann, *Nature* **342**, 643 (1989).
5. J. Boulter *et al.*, *Science* **249**, 1033 (1990); N. Nakanishi *et al.*, *Neuron* **5**, 569 (1990).
6. K. Keinänen *et al.*, *Science* **249**, 556 (1990).
7. An alternative nomenclature uses GluR-A, GluR-B, GluR-C, and GluR-D to refer to these subunits (6) and numbers the amino acids from the presumed  $\text{NH}_2$ -terminus of the final proteins, rather than from the presumptive initiator methionine.
8. M. Hollmann, M. Hartley, S. Heinemann, *Science* **252**, 851 (1991).
9. These experiments indicated that the region of GluR2 between amino acids 350 and 757 controls both the  $I$ - $V$  relation and the calcium permeability (R. Dingledine and R. I. Hume, unpublished observations).
10. The parent clones (GluR1, GluR2, GluR3) and all recombinant products were inserted into the plasmid Bluescript SK<sup>-</sup> (Stratagene). Single-stranded DNA template was rescued with VCSM13 helper phage (16), and site-directed mutations were made with the oligonucleotide-directed in vitro mutagenesis system version 2 (Amersham). The primers incorporated two nucleotide changes. One caused the desired change in amino acid sequence, whereas the second created a new restriction site for Eco RV without altering the amino acid sequence. *Escherichia coli* strain NM522 was transformed with the recombinant plasmids, and we verified the production of mutants by restriction site analysis and by sequencing through the mutant region.
11. *Xenopus* oocytes (stage V or VI) were injected with 2 to 25 ng of RNA transcribed in vitro by T3 RNA polymerase as described (4). We co-injected combinations of GluR1 and a second subunit at a ratio of

one to five to reduce the probability of the formation of homomeric GluR1 receptors. Voltage-clamp recordings with two electrodes were made 2 to 15 days after injection. For routine recording, oocytes were bathed in a solution containing 90 mM NaCl, 1 mM KCl, 1.7 to 1.8 mM MgCl<sub>2</sub>, 0.1 mM CaCl<sub>2</sub>, and 15 mM Hepes, pH 7.6. The low Ca<sup>2+</sup> concentration minimized the secondary activation of the Ca<sup>2+</sup>-dependent Cl<sup>-</sup> currents (17). Kainate was applied by bath perfusion. In most experiments, we used 300  $\mu$ M kainate to activate glutamate receptors, but lower concentrations were used on a few oocytes that produced large responses to 300  $\mu$ M kainate. We obtained *I-V* relations by applying 2-s voltage ramps (from -100 to +50 or +100 mV) in the presence and absence of kainate and then by subtracting the resting *I-V* curve from that observed in the presence of kainate.

12. We calculated slope conductance by measuring the current 5 mV positive and negative to the indicated potentials and dividing the difference by 10 mV.

13. Our substitution of Ba<sup>2+</sup> for Ca<sup>2+</sup> was not sufficient to abolish the secondary activation of the Ca<sup>2+</sup>-dependent Cl<sup>-</sup> current (18). In the experiments illustrated, we suppressed this current by including 0.4M EGTA as well as 3 M KCl in the recording and current pipettes and by keeping the application of kainate brief. We also achieved suppression of the

outward Cl<sup>-</sup> current by replacing all the extracellular Cl<sup>-</sup> with methanesulfonate (19) and including EGTA in the recording pipettes. For all combinations of subunits, the reversal potentials in the Cl<sup>-</sup>-containing and methanesulfonate-containing solutions were similar. In contrast to the records shown in Fig. 2, long applications of kainate (>15 s) often produced substantial outward currents in oocytes injected with any of the combinations of subunits that had inwardly rectifying *I-V* relations in low Ca<sup>2+</sup>, because of the secondary activation of the Cl<sup>-</sup> current.

14. The reversal potential for Cl<sup>-</sup> was estimated from tail currents following a depolarizing step that activated the Ca<sup>2+</sup>-dependent Cl<sup>-</sup> currents. In these experiments, the recording pipettes did not contain EGTA. The Cl<sup>-</sup> reversal potential was  $-25 \pm 1.8$  mV ( $n = 10$ ) in the high Ca<sup>2+</sup> solution and  $-32 \pm 2.8$  mV ( $n = 9$ ) in the high Ba<sup>2+</sup> solution.
15. Permeability ratios were calculated from the Goldman equation modified to include external divalent cations. In these calculations, it was assumed that anion permeability was negligible, that all monovalent cations were equally permeable, that intracellular monovalent cation concentration was 90 mM, and that the ion activities were 0.8 for monovalent cations and 0.5 for divalent cations. Calculations were made with and without compensation for the negative surface poten-

tial (20). The magnitude of this effect depends critically on the number and distribution of charges around the extracellular mouth of the channel, information not yet available. A surface charge equivalent to -20 mV at the channel would reduce the estimated permeability ratio of GluR1 plus GluR2(R607Q) receptors from 2.6 to 1.9.

16. J. Vieira and J. Messing, *Methods Enzymol.* **153**, 3 (1987).
17. M. E. Barish, *J. Physiol. (London)* **342**, 309 (1983); R. Miledi and I. Parker, *ibid.* **357**, 173 (1984).
18. R. Boton et al., *ibid.* **408**, 511 (1983).
19. N. Dascal, T. P. Snutch, H. Lübbert, N. Davidson, H. A. Lester, *Science* **231**, 1147 (1986).
20. C. Lewis, *J. Physiol. (London)* **286**, 417 (1979); P. Ascher and L. Nowak, *ibid.* **399**, 247 (1988).
21. T. A. Verdoorn, N. Burnashev, H. Monyer, P. H. Seeburg, B. Sakmann, *Science* **252**, 1715 (1991).
22. We thank M. Hollmann and L. Bolland for comments on the manuscript and J. Boulter, J. Egeberg, R. Duvoisin, I. Hermanns-Borgmeyer, and B. Bettler for advice and support throughout this study. Supported by NIH grants NS28709 (S.F.H.), NS25782 and NS21043 (R.I.H.), and NS27452 (R.D.), by the Klingenstein foundation, and by a gift from Bristol-Myers Squibb (R.D.).

3 May 1991; accepted 13 June 1991

## HRR25, a Putative Protein Kinase from Budding Yeast: Association with Repair of Damaged DNA

MERL F. HOEKSTRA,\* R. MICHAEL LISKAY, ALAN C. OU, ANTHONY J. DEMAGGIO, DAVID G. BURBEE, FRED HEFFRON

In simple eukaryotes, protein kinases regulate mitotic and meiotic cell cycles, the response to polypeptide pheromones, and the initiation of nuclear DNA synthesis. The protein HRR25 from the budding yeast *Saccharomyces cerevisiae* was defined by the mutation *hrr25-1*. This mutation resulted in sensitivity to continuous expression of the HO double-strand endonuclease, to methyl methanesulfonate, and to x-irradiation. Homozygotes of *hrr25-1* were unable to sporulate and disruption and deletion of *HRR25* interfered with mitotic and meiotic cell division. Sequence analysis revealed two distinctive regions in the protein. The NH<sub>2</sub>-terminus of HRR25 contains the hallmark features of protein kinases, whereas the COOH-terminus is rich in proline and glutamine. Mutations in *HRR25* at conserved residues found in all protein kinases inactivated the gene, and these mutants exhibited the *hrr25* null phenotypes. Taken together, the *hrr25* mutant phenotypes and the features of the gene product indicate that *HRR25* is a distinctive member of the protein kinase superfamily.

THE REPAIR OF DNA DAMAGE requires the coordination of a large number of gene products (1). For example, in responding to ultraviolet (UV) irradiation, cells can use photoreactivation or excision repair functions to correct genetic lesions. The repair of strand breaks, such as those created by x-rays, can proceed through recombinational mechanisms.

Many forms of DNA damage cause cells to arrest in G2 (2). During this G2 arrest, DNA lesions are repaired to ensure chromosomal integrity before mitotic segregation. In eukaryotes such as *S. cerevisiae*, genetic studies have defined repair-deficient mutants and have identified more than 50 radiation-sensitive (*RAD*) mutants with defects in genes that function in repair of damaged DNA (3).

To understand the functions involved in recognizing and repairing a broken chromosome, we have isolated mutants sensitive to continuous expression of the *HO* gene, which codes for a 65-kD site-specific endonuclease that cuts double-stranded DNA and initiates mating-type interconversion (4). The products of at least three DNA repair genes (*RAD51*, *RAD52*, and

*RAD54*) are required for the repair of the HO-created double-strand break (3, 5). However, the characteristics of the proteins encoded by these genes are not known (6). In a yeast strain containing a galactose-inducible *HO*, we identified mutants that were unable to grow on galactose. Of the mutants that were subsequently complemented by various galactose metabolism (*gal*) mutants, several showed varying sensitivity to the radiomimetic alkylating agent methyl methanesulfonate (MMS). Five alleles of known *rad* mutations were identified in this screen (7), and one mutation, *hrr25-1* (*HO* and radiation repair), displayed severe defects in DNA repair.

The *hrr25-1* mutation conferred a recessive DNA repair defect that included sensitivity to MMS (Fig. 1). The *hrr25-1* strains also showed sensitivity at 5 to 20 krad of x-irradiation (8), similar sensitivity to that observed with mutations in the radiation repair genes *RAD50* and *RAD52* (3, 6). These *hrr25-1* strains are no more sensitive to UV irradiation than are wild-type strains and are not temperature-sensitive for growth at 37°C. Although some *rad* mutants have several of the *hrr25-1* DNA repair phenotypes, *hrr25-1* strains differ in that they undergo nearly normal mitotic recombination (3, 9). Frequencies of spontaneous mitotic gene conversion and crossing-over were similar for homozygous *hrr25-1* and wild-type strains (Table 1). However, *HRR25* is required for the correct completion of meiosis. Homozygotes of *hrr25-1* showed fewer than 0.5% spores under conditions in which an isogenic wild-type strain sporulated to 75 to 85%. The *hrr25-1* mutation could be complemented by a number

M. F. Hoekstra, A. C. Ou, A. J. DeMaggio, D. G. Burbree, Molecular Biology and Virology Laboratory, The Salk Institute for Biological Studies, La Jolla, CA 92037.  
R. M. Liskay, Department of Therapeutic Radiology, Yale University School of Medicine, New Haven, CT 06510.  
F. Heffron, Department of Microbiology and Immunology, Oregon Health Sciences University, Portland, OR 97201.

\*To whom correspondence should be addressed.